Dalton Transactions

PAPER

View Article Online
View Journal | View Issue

CrossMark click for updates

Cite this: *Dalton Trans.*, 2016, **45**, 6619

Sedaxicenes: potential new antifungal ferrocene-based agents?†

R. Rubbiani,* O. Blacque and G. Gasser*

Received 28th October 2015,
Accepted 26th February 2016

DOI: 10.1039/c5dt04231c

www.rsc.org/dalton

Fungal infections are a group of diseases spread all over the world with an extremely high morbidity. Worryingly, although several pathogenic fungi were found to develop resistance towards traditional therapy, research towards the discovery of novel antimycotic agents is very limited. Considering the promising results obtained with the ferrocene-based drug candidates Ferroquine and Ferrocifen as antimalarial and anticancer drug candidates, respectively, we envisaged derivatizing the organic scaffold of a new broad-spectrum fungicide, namely sedaxane, with a ferrocenyl moiety in order to obtain new metal-based antifungal agents. The new ferrocenyl sedaxane derivatives called herein *Sedaxicenes* (**1a**, **2** and **3**) were characterized using different analytical techniques and the structures were confirmed by X-ray crystallography. As expected for antimycotic agents, **1a**, **2** and **3** were found to have a low or even no toxicity towards human cells (IC_{50} > 100 μM). Interestingly, while the parent drug did not display any mycotoxicity (EC_{50} > 100 μM), complex **1a** was found to have some antifungal activity with an IC_{50} value of 43 μM under the same experimental conditions. In order to investigate the possible redox-mediated mode of action of **1a**, we synthesized the ruthenocene analogue of **1a**, namely **1b**. Ruthenocene is known to have a completely different electrochemical behaviour from ferrocene although both the compounds are isostructural. As anticipated, complex **1a** was found to induce an increase of the reactive oxygen species level in *S. cerevisiae*, contrary to its **1b** analogue and to the parent compound sedaxane.

Introduction

Fungal infections are provoked by tiny parasites present in water, soil, plants, invertebrates and mammals called fungi.[1] Fungi belong to a broad family of eukaryotes which display features at the crossroads between mammalian cells and bacteria.[2–4] Like eukaryotes, they possess the genetic material located in the nucleus, mitochondria, an endoplasmic reticulum and a digestion vacuole system. Similar to bacteria, they are a spore-producing microorganism.[2–4] Fungi also have a characteristic cell wall responsible for nutrient trafficking with the host or the environment and with a protective function.[5]

Despite their limited mortality (<10 million per year), fungi displayed a very alarming morbidity.[6] For example, the lifetime incidence of candidiasis (fungal infections provoked by the *Candida* yeast family) in women reaches 75% and the recent data showed that 25% of the whole world population is affected by *Tinea pedis* (a mold responsible for the "ringworm of the foot").[6] This represents several hundred millions of infections per year, a number comparable to those of serious pathologies like malaria (data of the World Health Organization, WHO, updated December 2014). Notably, new diseases linked to new human life conditions (*e.g.* diabetes, obesity, cancer) enable pathogenic fungi to cause severe complications. Fungal infections are therefore involved in the worsening of other diseases, impacting the economic system of different nations. In the worst cases, they lead to human death.[7] Surprisingly, conventional therapies against fungi rely on a very limited number of drugs. These therapeutic agents were discovered in the last century and just 7 of them are nowadays in the list of WHO – Essential Medicine (data of October 2013).[8] Moreover, antifungal research is stagnant, especially if compared to other pathologies. In the last few decades, just a few new antifungal agents have been unveiled and they were mainly based on structural modifications of the already discovered active drugs. Worryingly, there have recently been an increasing number of reports showing that different pathologi-

Department of Chemistry, University of Zurich, Winterthurerstrasse 190, 8057 Zurich, Switzerland. E-mail: riccardo.rubbiani@chem.uzh.ch, gilles.gasser@chem.uzh.ch; Fax: +41-44-635-68-02; Tel: +41-44-635-46-86, +41-44-635-46-30

†Electronic supplementary information (ESI) available: Analytical data and crystal representation of **1a**, **2** and **3** (Fig. S1–S5); crystal data refinement and bond/angle calculations for complex **1** (Tables S1–S7); crystal data refinement and bond/angle calculations for complex **2** (Tables S9–S118); crystal data refinement and bond/angle calculations for complex **3** (Tables S19–S22); general crystal experiment settings and an example of antifungal toxicity in a 12-well plate (Fig. S6). CCDC 1433288–1433290. For ESI and crystallographic data in CIF or other electronic format see DOI: 10.1039/c5dt04231c

cal fungal strains are developing resistance against conventional therapy.[9] This alarming observation is a strong incentive for the discovery of novel compounds or strategies to fight this clearly underestimated problem.

Research on the medicinal potential of metal complexes has witnessed a very rapid growth in the last few decades. Platinum- and gadolinium-based compounds are nowadays heavily used as anticancer and imaging agents, respectively. Other metal complexes like Ferroquine (containing iron) or KP1339 (containing ruthenium) are in clinical trials.[10] The reason behind this "success story" is that metal complexes present very favourable features, which make them, in some cases, superior to organic compounds. For example, metal complexes display an enhanced stereochemistry and reactivity compared with organic molecules and can have a large repertoire of physico-chemical properties (lipophilicity, redox potential, *etc.*).[10,11] Surprisingly, there are only a limited number of studies on the activity of metal complexes [Co(II), Ni(II), Cu(II), Mn(I), Pd(II) Bi(III) complexes made a variety of ligands (*e.g.* azole moieties, thiosemicarbazones, carboxamides, indoles)] against fungal strains, hence leaving this very field pretty much unexplored.[12] Due to the encouraging results obtained by many research groups on the biological potential of metallocenes,[12,13] we recently embarked on a project to design novel metal-based antifungal agents. The synthesis, characterisation and biological evaluation of three new organometallic complexes based on a known fungicide are herein reported.

Results and discussion

Drug design

Recently, a potent broad-spectrum fungicide, namely sedaxane (ISO common name, CAS no. 874967-67-6, see Scheme 1 for chemical structure), was approved as a pesticide.[15] Sedaxane efficiently inhibits the fungal enzyme succinate dehydrogenase involved in the fungal oxidative phosphoryalation.[15] Of utmost interest is the fact that sedaxane displayed low toxicity and good clearance, with the majority of the drug excreted within 24 h (in mice models). Moreover, no oral, inhaling or dermal toxicity was observed for concentrations below 5 g per kg per day.[14] Interestingly, there are no studies on the possible application of sedaxane to fight human fungal infections.

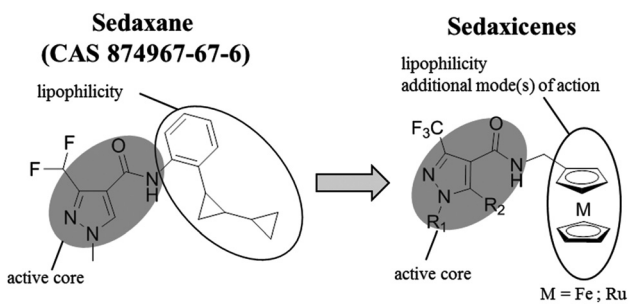

Scheme 1 Structures of sedaxane and sedaxicenes. The role of each unit in the molecules is described.

Motivated by the work of several research groups which derivatized a known drug with a ferrocenyl moiety to obtain a synergistic increase in activity (*e.g.* Ferrocifen, Ferroquine, ferrocenyl praziquantel, ferrocenyl platensimycin, *etc.*),[10,11] we envisaged coupling the favourable therapeutic profile of sedaxane with the potential of the ferrocenyl group (see Scheme 1).[12,13]

In this work, the core of sedaxane was modified at the bicycloprop-2-yl group, replacing it with a methylferrocene moiety. This replacement was assumed to not influence the overall bioactivity, which is hypothesized to be carried out by the pyrazole carboxamide group by interacting with the iron cluster of the active site of the enzyme.[14] Additionally, the presence of the ferrocenyl group was anticipated to afford a potential synergistic mode(s) of action due to the presence of a redox moiety. It was, for example, demonstrated by Biot and co-workers that the presence of the ferrocenyl moiety in Ferroquine was allowing for the formation of $^{\bullet}OH$. Since chloroquine cannot produce $^{\bullet}OH$, this radical generation was assumed to be responsible for the activity of Ferroquine on chloroquine-resistant parasite strains.[12,13] To further confirm the contribution of redox activity to the overall antifungal profile of our ferrocenyl derivatives, we synthesized a ruthenocenyl sedaxane analogue (**1b**, see Scheme 1). Ruthenocene is isostructural to ferrocene but has a significantly different electrochemical behaviour. This difference was shown in the past to play an important role in the formation or not of ROS by Biot and co-workers (*e.g.* the ruthenocene analogue of Ferroquine, namely Ruthenoquine was not producing ROS while Ferroquine was).[13] Of note is that different alkylic moieties were also inserted into the pyrazole core to have a small structure activity relationship (SAR) study.

Synthetic procedures

The synthesis of the metallocenyl analogues of sedaxane, that we have named sedaxicenes, was performed according to the established protocols (see Scheme 2).[16] The products **1a**, **1b**, **2** and **3** were all obtained in moderate yields (23–58%). The new

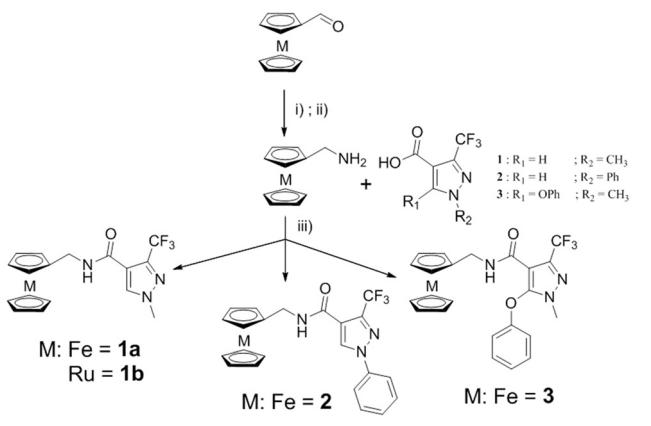

Scheme 2 Synthesis of the new antifungal ferrocenyl drug candidates; (i) NH_2OH in EtOH under reflux for 4 h; (ii) $LiAlH_4$ in THF under reflux for 3 h, (iii) DIPEA, HATU in DMF at room temperature for 24 h.

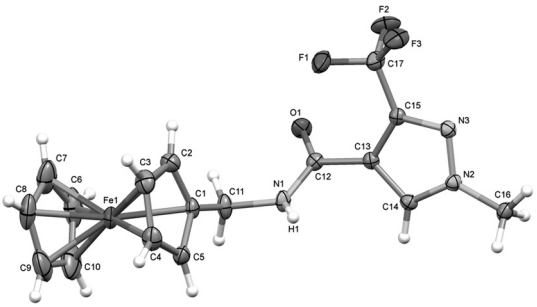

Fig. 1 X-ray crystal structure of **1a** with selective atomic numbering scheme. Thermal ellipsoids are drawn at the 30% probability level.

complexes were characterized by ^{1}H, ^{13}C and ^{19}F NMR spectroscopy as well as ESI-MS and X-ray diffraction studies, and their purity was assessed by elemental analysis (<0.5% from the calculated value).

The X-ray diffraction studies were performed on suitable single crystals which were obtained after slow evaporation of a concentrated solution of the complex in chloroform at 25 °C over a few days. The exemplar perspective view of the molecular structure of complex **1a** is shown in Fig. 1 (see the ESI† for the molecular structures of **2** and **3**). Specific features that confirmed the presence of the products were the disappearance of the acidic proton signal between 12.5 and 13.0 ppm in the ^{1}H NMR spectra, the up-field shift of the carbonyl carbon from ~190 ppm to ~160 ppm in the ^{13}C NMR spectra, the presence of a single signal in the ^{19}F NMR spectra and the M^{+} peak in the mass spectra.

Host cytotoxicity

With the steady increase of mycoses, antifungal agents are required to be often administered both topically and systemically, and to lack therefore host toxicity. In order to investigate the impact of our sedaxicenes on the host organism, **1a**, **2** and **3** were tested for their cytotoxicity against human cells *in vitro*. For these experiments, two cells lines were chosen, namely human fibroblast (MRC-5) and retinal pigment epithelial (RPE1 hTert), representing both superficial and internal cells, respectively. The influence of the metal complexes on the cellular proliferation was aimed to provide important information on the efficacy of the sedaxicenes as topical as well as systemic drug candidates. Sedaxane was used as a reference for comparative purposes and Clotrimazole as a positive control (see Table 1). As expected, sedaxane did not affect the cell viability. Complexes **1b**, **2** and **3** showed a very mild toxicity, in the mid-micromolar range (towards both the cell lines for **2** and just towards MRC-5 for **1b** and towards RPE for **3**). Remarkably, complex **1a** did not display any activity towards both cell lines. Interestingly, Clotrimazole was found to have a higher cytotoxicity than all sedaxicenes, with IC_{50} values in the low micromolar range.

Antifungal activity

Once established that the sedaxicenes had no or only minor toxicity towards human cell lines, the antifungal profile of these metal complexes was evaluated. *Saccharomyces cerevisiae* (SC) was chosen as a valid fungus model for preliminary biological evaluation.[17] The wild type colony of SC was cultured and diluted to reach the beginning of the growing phase just before treatment. SC was then seeded at different concentrations on the agar terrain poured into a 12-well plate and pre-treated with different concentrations of the target sedaxicenes. The plates were then incubated for 24 h at 30 °C and the colony formation was monitored *via* an Alpha Digitec camera with white light excitation. Sedaxane was used in the study for comparative purposes and Clotrimazole as a positive control.

Table 1 Antiproliferative effects on non-tumorigenic human fibroblast and human retinal pigment epithelial cell lines and antifungal activity of SC seeded on the agar terrain of **1ab–3**; sedaxane was used for comparative purposes and Clotrimazole as a positive control; values expressed in IC_{50}/EC_{50} (μM)

Compound	Human cell lines		*S. Cerevisiae*
	MRC-5	RPE	(OD = 0.02)
Clotrimazole	35.8 ± 3.5	13.3 ± 0.6	0.66 ± 0.26
Sedaxane	>100	>100	>100
Complex **1a**	>100	>100	43.3 ± 6.2
Complex **1b**	41.0 ± 5.3	>100	>100
Complex **2**	48.9 ± 3.1	50.5 ± 7.9	98.6 ± 1.7
Complex **3**	>100	67.8 ± 9.4	91.9 ± 3.6

Complexes **1a**, **2** and **3** were found to reduce the colony formation of SC, displaying moderate IC_{50} values in the mid-high micromolar range. Complex **1a**, bearing a less hindered pyrazole ring in comparison with **2** and **3**, was the most active throughout the series with an EC_{50} value of 43 μM (see Table 1 and Fig. 2 for an exemplar depicted experiment). Interestingly, sedaxane as well as **1b** did not display any activity up to the highest concentration used in this study (100 μM).

Reactive oxygen species evaluation

The drug design of the sedaxicenes was based on the insertion of a ferrocenyl moiety into the known broad-spectrum fungicide sedaxane. The rationale behind this approach is that the redox iron centre could improve the therapeutic profile of sedaxane with (an) additional mode(s) of action. Complex **1a** displayed the best antimycotic profile of all compounds tested

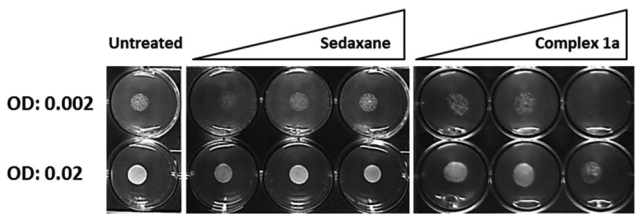

Fig. 2 SC growth inhibition upon treatment with increasing concentrations of sedaxane and complex **1a** (exemplary figures concerning **1b**, **2**, **3** and Clotrimazole are reported in the ESI†); experiment performed at different SC growing indexes (OD = 0.002 and 0.02, respectively).

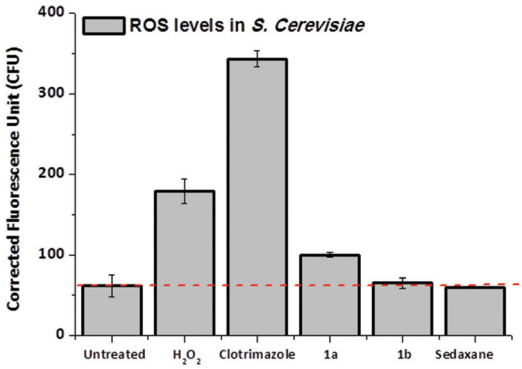

Fig. 3 ROS level determination in SC upon treatment with complex **1a** and **1b**; sedaxane (100 μM) was used for comparative purposes, H_2O_2 (10 μM) and Clotrimazole (5 μM) as a positive control.

in this study. In order to assess the possible redox activity of complex **1a**, we investigated the rise of the reactive oxygen species (ROS) level in fungal culture upon treatment with this compound and compared the data with sedaxane (as parent drug) and **1b** (as redox inactive **1a** analogue). For this purpose, the cell-permeable dye 2′,7′-dichlorofluorescein di-acetate (H_2DCF-DA), which turns to be highly fluorescent upon oxidation in the presence of ROS, was used, as previously reported by our group for a cytotoxic Au(III) complex.[18] Hence, SC culture was treated for 16 h with 100 μM of complexes **1a** and **1b**. The medium was then replaced with fresh YPD (not containing the metal compounds) treated with H_2DCF-DA. The SC culture was further incubated for 1 h, allowing for the internalization of the dye before the ROS level was quantified. Strikingly, the ROS level in SC treated with complex **1a** displayed an increase of 33% in comparison with the untreated control (see Fig. 3). This effect was not observed in the case of **1b**. SC treated with sedaxane showed a similar ROS level than the basal value, suggesting that the ferrocenyl moiety is playing indeed a pivotal role to achieve a valuable fungicidal profile.

Experimental

General

Chemicals and reagents. All chemicals were of reagent grade quality or better, obtained from commercial suppliers and used without further purification. Sedaxane has been provided by Syngenta AG. Solvents were used as received or dried over molecular sieves. All preparations were carried out using standard Schlenk techniques.

Instrumentation and methods. ^{1}H, ^{19}F and ^{13}C NMR spectra were recorded in deuterated solvents on 400 (1H, 400 MHz; 13C, 100.6 MHz) or 500 (1H, 500 MHz; 13C, 126 MHz) MHz spectrometers at room temperature. The chemical shifts δ, are reported in ppm (parts per million). The residual solvent peaks have been used as an internal reference. The abbreviations for the peak multiplicities and signals groups are as follows: s (singlet), d (doublet), dd (doublet of doublets), t (triplet), q (quartet), m (multiplet), br (broad) Ar (aromatic) and Py (pyrazole). ESI-MS and UPLC-MS were obtained with a Bruker Esquire 6000 mass spectrometer. LC-MS and UPLC-MS spectra were recorded on an Acquity Waters system equipped with a PDA detector and an auto sampler using an ACQUITY UPLC BEH C18 Gravity 1.7 μm (2.1 mm × 50 mm) reverse phase column. A total of 2 μL of the solution was injected into the UPLC that was connected to a mass spectrometer operated in ESI mode. The UPLC runs (flow rate 0.6 mL min^{-1}) were performed with a linear gradient of A (acetonitrile (Sigma-Aldrich HPLC-grade)) and B (distilled water containing 0.1% formic acid): t = 0–0.25 min, 5% A; t = 1.5 min, 100% A; t = 5.0 min, 100% A. Elemental micro-analyses were performed on a LecoCHNS-932 elemental analyser

Synthesis

Methylaminoferrocene. Methylaminoferrocene was synthesized as previously reported.[16] Experimental data matched with the literature reports.

General procedure for synthesis of the sedaxicenes. The opportune carboxylic acid (0.26 mmol) was dissolved in dry DMF (2 mL) under a N_2 atmosphere. This solution was added to a 1 mL solution of *N*,*N*′-diisopropylethylamine (DIPEA, 0.37 mmol) and 1-[bis(dimethylamino)methylene]-1*H*-1,2,3-triazolo[4,5-*b*]pyridinium 3-oxid hexafluorophosphate (HATU) (0.50 mmol) in dry DMF. The new solution was then stirred for 20 min at room temperature. Methylaminoferrocene (56 mg, 0.26 mmol) dissolved in 10 mL of dry DMF was then added to the mixture which was then stirred in the dark overnight. The solvent was evaporated using a high-vacuum pump. The reddish oil was then purified by column chromatography (silica, ethylacetate : hexane : acetone, 7 : 2 : 1, R_f = 0.70). The fractions were collected and the solvent was removed *in vacuo* to obtain yellow powder.

***N*-Methylferrocenyl,3-(trifluoromethyl)-1-methyl-1*H*-pyrazole-4-carboxylamide (complex 1a).** Yield 46% (47 mg). ^{1}H NMR (500 MHz), $CDCl_3$, δ (ppm) 7.93 (s, 1H, ArH), 6.20 (s, 1H, NH), 4.23 (m, 12H, FcH/CH_2), 3.95 (s, 3H, CH_3); ^{13}C NMR (500 MHz), $CDCl_3$, δ (ppm) 160.5, 136.5, 122.7, 120.6, 117.9, 100.9, 70.0, 69.5, 68.9, 40.5, 39.9; ^{19}F NMR (500 MHz), $CDCl_3$, δ (ppm) −59.6; MS (ESI+): m/z 391.1 $[M]^+$; elemental analysis (%) for $[C_{17}H_{16}F_3FeN_3O]$: calc. C: 52.20, H: 4.12, N: 10.74; found C: 52.25, H: 4.21, N: 10.59.

***N*-Methylferrocenyl,3-(trifluoromethyl)-1-phenyl-1*H*-pyrazole-4-carboxylamide (complex 2).** Yield 48% (57 mg). ^{1}H NMR (500 MHz), $CDCl_3$, δ (ppm) 8.48 (s, 1H, PyH), 7.70 (d, 2H, ArH), 7.50 (t, 2H, ArH), 7.41 (t, 1H, ArH), 6.33 (s, 1H, NH), 4.34 (d, 2H, CH_2), 4.23 (br, 2H, Fc), 4.20 (s, 5H, Fc), 4.18 (br, 2H, Fc); ^{13}C NMR (500 MHz), $CDCl_3$, δ (ppm) 160.2, 142.8, 139.2, 133.7, 130.4, 129.1, 120.6, 119.1, 100.9, 100.0, 98.1, 70.7, 40.2, 33.2; ^{19}F NMR (500 MHz), $CDCl_3$, δ (ppm) −59.7; MS (ESI+): m/z 453.1 $[M]^+$; elemental analysis (%) for $[C_{22}H_{18}F_3FeN_3O]$: calc. C: 58.30, H: 4.00, N: 9.27; found C: 57.81, H: 3.90, N: 8.77.

***N*-Methylferrocenyl,1-methyl-5-phenoxy-3-(trifluoromethyl)-1*H*-pyrazole-4-carboxylamide (complex 3).** Yield 23% (29 mg).

^{1}H NMR (500 MHz), $CDCl_3$, δ (ppm) 7.38 (t, 2H, ArH), 7.20 (t, 1H, ArH), 6.21 (s, 1H, NH), 4.11 (m, 9H, Fc), 4.05 (s, 2H, CH_2), 3.68 (s, 3H, CH_3); ^{13}C NMR (500 MHz), $CDCl_3$, δ (ppm) 159.0, 156.1, 148.6, 131.2, 125.6, 119.9, 115.9, 105.9, 101.3, 100.2, 99.3, 98.1, 69.4, 39.3, 36.1; ^{19}F NMR (500 MHz), $CDCl_3$, δ (ppm) −62.2; MS (ESI+): m/z 483.1 $[M]^+$; elemental analysis (%) for $[C_{23}H_{20}F_3FeN_3O_2]$: calc. C: 57.16, H: 4.17, N: 8.70; found C: 57.01, H: 4.09, N: 8.59.

***N*-Methylruthenocenyl,3-(trifluoromethyl)-1-methyl-1*H*-pyrazole-4-carboxylamide (complex 1b).** Ruthenocene carboxylaldheyde[16] (130 mg, 0.5 mmol) was dissolved in 10 mL of absolute ethanol. To this mixture was then added hydroxylamine hydrochloride (64 mg, 1.5 mmol) and an excess of NaOH (5 mmol). The resulting mixture was refluxed for 3 h under a N_2 atmosphere. The obtained ruthenocenyl oxyme was extracted with CH_2Cl_2, washed with bidistilled water, dried on $MgSO_4$ and, after filtration, the organic solvent was evaporated under reduced pressure. Ruthenocenyl oxyme was directly used without further purification for the next synthetic step.

Ruthenocenyl oxyme was then dissolved in dry 5 mL of THF and reduced to methylaminoferrocene in the presence of $LiAlH_4$ (190 mg, 5 mmol) under reflux conditions for 6 h under a N_2 atmosphere. The mixture was cooled down and hydrolyzed with 20 mL of bidistilled water. Methylaminoruthenocene was then extracted with diethylether. The combined organic layers were then removed under reduced pressure.

3-(Trifluoromethyl)-1-methyl-1*H*-pyrazole-4-carboxylic acid (0.50 mmol) was dissolved in dry DMF (2 mL) under a N_2 atmosphere. This solution was added to a 1 mL solution of *N*,*N*′-diisopropylethylamine (DIPEA, 1.5 mmol) and 1-[bis-(dimethylamino)methylene]-1*H*-1,2,3-triazolo[4,5-*b*]pyridinium 3-oxid hexafluorophosphate (HATU) (1.5 mmol) in dry DMF. The new solution was then stirred for 20 min at room temperature. Methylaminoruthenocene dissolved in 10 mL of dry DMF was then added to the mixture which was then stirred in the dark overnight. The solvent was evaporated using a high-vacuum pump. The reddish oil was then purified by column chromatography (silica, ethylacetate : hexane, 8 : 2, R_f = 0.75). The fractions were collected and the solvent was removed *in vacuo* to obtain a brownish powder. Yield 58%. ^{1}H NMR (500 MHz), $CDCl_3$, δ (ppm) 7.91 (s, 1H, ArH), 6.10 (s, 1H, NH), 4.59 (m, 2H, RcH) 4.50 (m, 5H, RcH), 4.49 (m, 2H, RcH), 4.13 (d, 2H, CH_2), 3.93 (s, 3H, CH_3); ^{13}C NMR (500 MHz), $CDCl_3$, δ (ppm) 160.6, 136.3, 122.7, 120.6, 117.9, 89.0, 71.2, 70.8, 70.5, 40.4, 39.4; ^{19}F NMR (300 MHz), $CDCl_3$, δ (ppm) −55.8; MS (ESI+): m/z 438.1 $[M + H]^+$, 896.1 $[2M + Na]^+$; elemental analysis (%) for $[C_{17}H_{16}F_3RuN_3O]$: calc. C: 46.79, H: 3.70, N: 9.63; found C: 46.83, H: 3.73, N: 9.90.

Crystallographic data collections and structure refinements

Single-crystal X-ray diffraction data were collected at 183(1) K on an Agilent Technologies SuperNova diffractometer for **1a–2** and on an Agilent Technologies Xcalibur Ruby area-detector diffractometer for **3** using a single wavelength Enhance X-ray source with Mo K_α radiation (λ = 0.71073 Å) for **1a** and **3** or with Cu K_α radiation (λ = 1.54184 Å) for **2** from a micro-focus X-ray source, and an Oxford Instrument's Cryojet XL cooler. The selected suitable single crystal was mounted using polybutene oil on a flexible loop fixed on a goniometer head and immediately transferred to the diffractometer. Pre-experiment, data collection, data reduction and analytical absorption correction[19] were performed with the program suite CrysAlisPro.[19] Using Olex2,[19] the structures were solved with the ShelXS97[19] structure solution program using direct methods and refined with the SHELXL2014[19] program package by full-matrix least-squares minimization on F^2. PLATON[19] was used to check the result of the X-ray analyses. All non-H atoms were anisotropically refined. All hydrogen positions were calculated after each cycle of refinement using a riding model with C–H = 0.93 Å and U_{iso}(H) = 1.2U_{eq}(C) for aromatic H atoms, with C–H = 0.97 Å and U_{iso}(H) = 1.2U_{eq}(C) for methylene H atoms, and with C–H = 0.96 Å and U_{iso}(H) = 1.5U_{eq}(C) for methyl H atoms, except for the amido H atoms which were freely refined. For more details about the data collection and refinements parameters, see the Crystallographic Information files (ESI†). Crystal data for $C_{17}H_{16}F_3FeN_3O$ (**1a**) (M = 391.18 g mol^{-1}): orthorhombic, space group *Pbca* (no. 61), a = 10.3579(2) Å, b = 8.72054(14) Å, c = 36.8998(7) Å, V = 3333.04(10) Å^3, Z = 8, T = 183(1) K, μ(MoKα) = 0.946 mm^{-1}, D_{calc} = 1.559 g cm^{-3}, 22 551 reflections measured (4.416° ≤ 2Θ ≤ 50.692°), 3034 unique (R_{int} = 0.0293, R_{sigma} = 0.0172) which were used in all calculations. The final R_1 was 0.0380 ($I > 2\sigma(I)$) and wR_2 was 0.0929 (all data). Crystal data for $C_{22}H_{18}F_3FeN_3O{\cdot}CHCl_3$ (**2**) (M = 572.61 g mol^{-1}): monoclinic, space group *I*2/a (no. 15), a = 10.6241(2) Å, b = 15.1983(4) Å, c = 29.6784(7) Å, β = 90.352(2)°, V = 4792.03(19) Å^3, Z = 8, T = 183(1) K, μ(CuKα) = 8.534 mm^{-1}, D_{calc} = 1.587 g cm^{-3}, 16 614 reflections measured (5.956° ≤ 2Θ ≤ 136.496°), 4393 unique (R_{int} = 0.0432, R_{sigma} = 0.0284) which were used in all calculations. The final R_1 was 0.0370 ($I > 2\sigma(I)$) and wR_2 was 0.0994 (all data). Crystal data for $C_{23}H_{20}F_3FeN_3O_2$ (**3**) (M = 483.27 g mol^{-1}): triclinic, space group $P\bar{1}$ (no. 2), a = 9.4458(3) Å, b = 10.3520(4) Å, c = 11.0470(4) Å, α = 96.727(3)°, β = 102.651(3)°, γ = 100.958(3)°, V = 1020.46(6) Å^3, Z = 2, T = 183(1) K, μ(MoKα) = 0.793 mm^{-1}, D_{calc} = 1.573 g cm^{-3}, 24870 reflections measured (4.534° ≤ 2Θ ≤ 61.016°), 6226 unique (R_{int} = 0.0381, R_{sigma} = 0.0276) which were used in all calculations. The final R_1 was 0.0344 ($I > 2\sigma(I)$) and wR_2 was 0.0941 (all data). CCDC 1433288 (for **1**), 1433289 (for **2**), and 1433290 (for **3**) contain the supplementary crystallographic data for this paper.

Biological evaluation

Cell culture. Human fibroblast (MRC-5) and retinal pigment epithelial (RPE) cell lines were cultured in F-10 medium supplemented with 10% fetal calf serum (FCS, Gibco), 100 U per mL penicillin, 100 μg per mL streptomycin or DMEM medium (Gibco) supplemented with 10% fetal calf serum (FCS, Gibco), 100 U per mL penicillin, and 100 μg per mL streptomycin, respectively, at 37 °C and 6% CO_2.

Yeast culture. Wild type *Saccharomyces cerevisiae* was freshly inoculated and cultured in autoclaved YPD buffer containing 2% bacto peptone, 1% bacto yeast extract and 2% glucose anhydrous at 30 °C (Kuhner shaker Labtherm, Kuhner Switzerland).

Cytotoxicity studies. Cytotoxicity studies of the effect of **1ab–3** were performed by a fluorometric cell viability assay using resazurin (Promocell GmbH).[18] Briefly, one day before treatment the cells were plated in triplicate in 96-well plates at a density of 4×10^3 cells per well in 100 μL. Upon treating the cells with increasing concentrations of the new sedaxicenes, the cells were incubated for 48 h at 37 °C/6% CO_2, the medium was removed, and 100 μL of complete medium containing resazurin (0.2 mg mL^{-1} final concentration) was added. After 4 h of incubation at 37 °C/6% CO_2, the fluorescence of the highly red fluorescent resorufin product was quantified at 590 nm emission with 540 nm excitation wavelength using a SpectraMax M5 Microplate Reader. The results were expressed as mean ± standard deviation error of independent experiments.

Toxicity towards fungi. The activity of complex **1ab–3** on SC was evaluated *via* a newly established colony formation assay. Briefly, one day before treatment an aliquot of wild type SC was inoculated in 5 mL YPD buffer solution (see above) and incubated overnight at 30 °C. The fungal proliferation was then quantified at 600 nm in a Cary60 UV/Vis (Agilent Technologies). The SC was then seeded at different concentrations of the yeast (representing OD of 0.02 for mid-growth colony and 0.002 for low-growth colony) in 12-well plates containing a 2 mL growing terrain. The growing terrain was composed of YPD containing 2% of agar, autoclaved and kept at 50 °C (water bath, Kotterman AG). Just before use, the growing terrain was treated with increasing concentrations of the new sedaxicenes and poured in different wells, before solidification. The treated plates were loaded with SC and incubated for 24 h at 30 °C. The fungal colony formation was monitored with an Alpha Digitec camera (Bucher Biotec) and the colony density was calculated with AlphaImager software (v1.3.0.7) with multiplex band analysis mode/single tool. A series of blanks (with the terrain not seeded with SC), a negative control (with the terrain seeded with SC and treated just DMSO as vehicle) and Clotrimazole as a positive control were performed. The results were expressed as mean ± standard error of independent experiments.

ROS level determination. The evaluation of intracellular ROS levels was performed following a method recently established by our group and re-adapted for fungal cultures.[18] The ROS determination was detected by the use of 2′,7′-dichlorofluorescin diacetate (H_2DCF-DA, Sigma-Aldrich), a cell-permeable non-fluorescent probe which is hydrolyzed in cells and, which upon oxidation turns to highly fluorescent 2′,7′ dichlorofluorescein.[18] Briefly, an aliquot of SC was inoculated in 5 mL YPD buffer one day before treatment and incubated at 30 °C under gentle shaking (180 rpm) in a Kuhner shaker Labtherm incubator (Kuhner, Switzerland) overnight. The culture was then diluted to an OD of 0.005, added with 100 μM of **1a–1b** and incubated for further 16 h. The YPD medium was then replaced with fresh medium containing H_2DCF-DA (final concentration 20 μM) and further incubated for 1 h at 30 °C under gentle shaking. The OD of the fungal growth was re-measured, the suspension was plated at different dilutions in duplicate in a 96-well plate and the fluorescence was quantified at 530 nm emission with 488 nm excitation wavelength using a SpectraMax M5 Microplate Reader. The results were expressed as mean and standard deviation error of different independent experiments, corrected for the fungal population. Sedaxane (100 μM) was used for comparative purposes and H_2O_2 at a final concentration of 10 μM and Clotrimazole at a final concentration of 5 μM as positive controls.

Conclusions

The invasiveness and aggressiveness of pathogenic fungi are too often underestimated or even ignored and have not been reflected in an adequate new drug output – the majority of the benchmark products were discovered in the last century! Worryingly, pathogenic fungi have started to develop drug tolerance, defeating an increasing number of therapies. Because of the incidence, resistance and health risk of fungi-related diseases, the discovery of novel drugs or strategies to fight fungal infections is highly necessary. In this article, we coupled a new effective fungicide, namely sedaxane, with ferrocenyl and ruthenocenyl moieties. This strategy has already been successfully employed in medicinal chemistry to increase the therapeutic potential of the accepted drugs. More specifically, we synthesised four new organometallic compounds (complexes **1a**, **1b**, **2** and **3**). The complexes were fully characterized by ^{1}H, ^{13}C and ^{19}F NMR spectroscopy, ESI-MS, elemental analysis (deviation < 0.5%) and X-ray crystallography (for the ferrocene derivatives **1a**, **2** and **3**). The four complexes were found to have a very low or even no toxicity towards human immortalized fibroblast or epithelial cells. This result is favourable in relation to topical as well as systemic applications. Complex **1a**, bearing a methyl group on the pyrazole core, was found to have an antifungal toxicity in the micromolar range contrary to **2** and **3**, which bear a phenyl or a phenoxy group on the pyrazole core, respectively. This fact suggests that structural modifications, which hinder the pyrazole ring of the compound, affect drastically the overall activity. Strikingly, investigation of the ROS level in SC upon treatment with **1a** and its isostructural but not redox-active ruthenocene analogue **1b** evidenced an increase of these noxious species for **1a** but not for **1b**. Moreover, it has to be noted that the parent drug sedaxane was found to not have any fungicidal profile and to not induce ROS formation under the same experimental conditions. It can therefore be assumed that the increase in mycotoxicity depends on the presence of the ferrocenyl moiety and its redox activity. Altogether these data represent a promising starting point for the development of new potent metal-based antifungal agents.

Acknowledgements

This work was financed by the Swiss National Science Foundation (Professorships PP00P2_133568 and PP00P2_157545 to G. G.), the University of Zurich (G. G.), the Stiftung für

wissenschaftliche Forschung of the University of Zurich (G. G.), the Novartis Jubilee Foundation (G. G. and R. R.), the Forschungskredit of the University of Zurich (R. R.) and the UBS Promedica Stiftung (G. G. and R. R.). The authors thank Syngenta AG for providing a sedaxane sample for the comparative biological experiments as well as Dr Murat Aykut and PD Dr Stefano Ferrari for helpful discussions.

References

1 P. N. Lipke and R. Ovalle, *J. Bacteriol.*, 1998, **180**, 3735–3740; D. A. Enoch, H. A. Ludlam and N. M. Brown, *J. Med. Microbiol.*, 2006, **55**, 809–818.
2 S. M. Bowman and S. J. Free, *BioEssays*, 2006, **28**, 799–808.
3 A. Caridi, *Antonie van Leeuwenhoek*, 2006, **89**, 417–422.
4 E. Barreto-Bergter, M. R. Pinto and M. L. Rodrigues, *An. Acad. Bras. Cienc.*, 2004, **76**, 67–84.
5 D. Gozalbo, M. V. Elorza, R. Sanjuran, A. Marcilla, E. Valentin and R. Sentandreu, *Pharmacol. Ther.*, 1993, **60**, 337–345; M. Debono and R. S. Gordee, *Annu. Rev. Microbiol.*, 1994, **48**, 471–497.
6 M. P. English and J. Turvey, *Br. Med. J.*, 1968, **4**, 228–230; S. Perea, M. J. Ramos, M. Garau, A. Gonzales, A. R. Norviega and A. Del Palacio, *J. Clin. Microbiol.*, 2000, **38**, 3226–3230; B. Havlickova, V. A. Czaika and M. Friedrich, *Mycoses*, 2008, **51**, 2–15; R. P. Hobson, *J. Hosp. Infect.*, 2003, **55**, 159–168.
7 D. A. Enoch, H. A. Ludlam and N. M. Brown, *J. Med. Microbiol.*, 2006, **55**, 809–818; J. Menzin, J. L. Meyers, M. Friedman, J. R. Korn, J. R. Perfect, A. A. Langston, R. P. Danna and G. Papadopoulos, *Am. J. Infect. Control*, 2011, **39**, 15–20.
8 M. A. Pfaller, *Am. J. Med.*, 2012, **125**, S3–S13; C. M. Martel, J. E. Parker, O. Bader, M. Weig, U. Gross, A. G. S. Warrilow, D. E. Kelly and S. L. Kelly, *Antimicrob. Agents Chemoter.*, 2010, **54**, 3578–3583; H. Hof, *Drug Resist. Updates*, 2008, **11**, 25–31.
9 T. Ohyama, S. Miyakoshi and F. Isono, *Antimicrob. Agents. Chemoter.*, 2004, **48**, 319–322.
10 G. Gasser and N. Metzler-Nolte, *Curr. Opin. Chem. Biol.*, 2012, **16**, 84–91; G. Jaouen, A. Vessieres and S. Top, *Chem. Soc. Rev.*, 2015, **44**, 8802–8817; C. H. Huang and A. Tsourkas, *Curr. Top. Med. Chem.*, 2013, **13**, 411–421; M. Patra, G. Gasser, M. Wenzel, K. Merz, J. E. Bandow and N. Metzler-Nolte, *Organometallics*, 2010, **29**, 4312–4319.
11 C. G. Hartinger, N. Metzler-Nolte and P. J. Dyson, *Organometallics*, 2012, **31**, 5677–5685; U. Schatzschneider and N. Metzler-Nolte, *Angew. Chem., Int. Ed.*, 2006, **118**, 1534–1537; M. Dorr and E. Meggers, *Curr. Opin. Chem. Biol.*, 2014, **19**, 76–81; I. Ott, *Coord. Chem. Rev.*, 2009, **253**, 1670–1681; N. P. E. Barry and P. J. Sadler, *Chem. Commun.*, 2013, **49**, 5106–5131.
12 Y. Wang, P. Pigeon, S. Top, M. J. McGlinchey and G. Jaouen, *Angew. Chem., Int. Ed.*, 2015, **54**, 10230–10233; A. Nguyen, A. Vessieres, E. A. Hillard, S. Top, P. Pigeon and G. Jaouen, *Chimia*, 2007, **61**, 716–724; F. Dubar, T. J. Egan, B. Pradines, D. Kuter, K. K. Ncokazi, D. Forge, J. F. Paul, C. Pierrot, H. Kalamou, J. Khalife, E. Buisine, C. Rogier, H. Vezin, I. Forfar, C. Slomianny, X. Trivelli, S. Kapishnikov, L. Leiserowitz, D. Dive and C. Biot, *ACS Chem. Biol.*, 2011, **6**, 275–287; M. Barends, A. Jaidee, N. Khaohirun, P. Singhasivanon and F. Nosten, *Malar. J.*, 2007, **6**, 81; M. Patra, K. Ingram, V. Pierroz, S. Ferrari, B. Spingler, J. Keiser and G. Gasser, *J. Med. Chem.*, 2012, **55**, 8790–8798.
13 F. Dubar, C. Slomianny, J. Khalife, D. Dive, H. Kalamou, Y. Guerardel, P. Grellier and C. Biot, *Angew. Chem., Int. Ed.*, 2013, **52**, 7690–7693; F. Dubar, T. J. Egan, B. Pradines, D. Kuter, K. K. Ncokazi, D. Forge, J.-F. Paul, C. Pierroz, H. Kalamou, J. Khalife, E. Buisine, C. Rogier, H. Vezin, I. Forfar, C. Slomianny, X. Trivelli, S. Kapishnikov, L. Leiserowitz, D. Dive and C. Biot, *ACS Chem. Biol.*, 2011, **6**, 275–287; G. Gasser, *Chimia*, 2015, **69**, 442–446; J. Hess, J. Keiser and G. Gasser, *Future Med. Chem.*, 2015, **7**, 821–830; Y. C. Ong, V. L. Blair, L. Kedzierski and P. C. Andrews, *Dalton Trans.*, 2014, **43**, 12904–12916; M. Patra, M. Wenzel, P. Prochnow, V. Pierroz, G. Gasser, J. E. Bandow and N. Metzler-Nolte, *Chem. Sci.*, 2015, **6**, 214–224; M. Patra and G. Gasser, *ChemBioChem*, 2012, **13**, 1232–1252.
14 C. Biot, N. Francois, L. Maciejewski, J. Brocard and D. Poulain, *Bioorg. Med. Chem. Lett.*, 2001, **10**, 839–841; A. Garoufis, S. K. Hadikakou and N. Hadjiliadis, *Coord. Chem. Rev.*, 2009, **253**, 1384–1397; N. V. Loginova, T. V. Koval'chuk, N. P. Osipovich, G. I. Polozov, V. L. Sorokin, A. A. Chernyaskaya and O. I. Shadyro, *Polyhedron*, 2008, **27**, 985–991; M. B. Halli, R. S. Malipatil, R. B. Sumathi and K. Shivakumar, *Pharm. Lett.*, 2013, **5**, 182–188; M. Kaya, E. Demir and H. Bekci, *J. Enzyme Inhib. Med. Chem.*, 2013, **28**, 885–893; E. Pahontu, V. Fala, A. Gulea, D. Poirier, V. Tapcov and T. Rosu, *Molecules*, 2013, **18**, 8812–8836; E. Rodriguez-Fernandes, J. L. Manzano, J. J. Benito, R. Hermosa, E. Monte and J. J. Criado, *J. Inorg. Biochem.*, 2005, **99**, 1558–1572; V. S. Pore, M. A. Jagtap, S. G. Agalave, A. K. Pandey, M. I. Siddiqi, V. Kumar and P. K. Shukla, *MedChemComm*, 2012, **3**, 484–488; J. Li, T. Xi, B. Yan, Y. Guan, M. Yang, J. Song and H. Ma, *New J. Chem.*, 2015, DOI: 1039/c5nj01845e; P. V. Simpson, C. Nagel, H. Bruhn and U. Schatzschneider, *Organometallics*, 2015, **34**, 3809–3815.
15 R. Zeun, G. Scalliet and M. Oostendorp, *Pest Manage. Sci.*, 2013, **69**, 527–534; M. Yoshida, P. V. Shah and D. McGregor, *J. Med. Plants Res.*, 2012, 769–839; W. Donovan, Sedaxane – Food and Agriculture Organization report, 2012, 1827–1917; H. Walter, H. Tobler, D. Gribkov and C. Corsi, *Chimia*, 2015, **69**, 425–434.
16 M. Patra, J. Hess, S. Konatsching, B. Spingler and G. Gasser, *Organometallics*, 2013, **32**, 6098–6105; P. D. Beer and D. K. Smith, *Dalton Trans.*, 1998, 417–423; A. Baramee, A. Coppin, M. Mortuaire, L. Pelinski, S. Tomavo and J. Brocard, *Bioorg. Med. Chem.*, 2006, **14**, 1294–1302;

D. V. Muratov, A. S. Romanov and A. R. Kudinov, *Russ. Chem. Bull.*, 2014, **63**, 2485–2492.

17 M. E. Cardenas, M. C. Cruz, M. Del Poeta, N. Chung, J. R. Perfect and J. Heitman, *Clin. Microbiol. Rev.*, 1999, **12**, 583–611; H. Karathia, E. Vilaprinyo, A. Sorribas and R. Alves, *PLoS ONE*, 2011, **6**, e16015.

18 R. Rubbiani, T. N. Zehnder, C. Mari, O. Blacque, K. Venkatesan and G. Gasser, *ChemMedChem*, 2014, **9**, 2781–2790; M. Zhang, J. Shi and L. Jiang, *Electron. J. Biotechnol.*, 2015, **18**, 202–209; A. Leonidova, V. Pierroz, R. Rubbiani, Y. Lan, A. G. Schmitz, A. Kaech, R. K. O. Sigel, S. Ferrari and G. Gasser, *Chem. Sci.*, 2014, **5**, 4044–4056.

19 Agilent Technologies (formerly Oxford Diffraction), Yarnton, Oxfordshire, England, 2012; R. C. Clark and J. S. Reid, *Acta Crystallogr., Sect. A: Fundam. Crystallogr.*, 1995, **51**, 887; *CrysAlisPro, Version 1.171.36.20*, Agilent Technologies, Yarnton, Oxfordshire, England, 2012; O. V. Dolomanov, L. J. Bourhis, R. J. Gildea, J. A. K. Howard and H. J. Puschmann, *J. Appl. Crystallogr.*, 2009, **42**, 339; G. M. Sheldrick, *Acta Crystallogr.*, 2008, **A64**, 112; G. M. Sheldrick, *Acta Crystallogr.*, 2015, **A71**, 3; A. L. Spek, *J. Appl. Crystallogr.*, 2003, **36**, 7.